HHS Public Access

Author manuscript

Cell Host Microbe. Author manuscript; available in PMC 2019 February 14.

Published in final edited form as:

Cell Host Microbe. 2018 February 14; 23(2): 274–281.e2. doi:10.1016/j.chom.2017.12.006.

Tracking *Vibrio cholerae* cell-cell interactions during infection reveals bacterial population dynamics within intestinal microenvironments

Yang Fu[1,2], **Brian T. Ho**[1,2], and **John J. Mekalanos**[1,3,*]

[1]Department of Microbiology and Immunobiology, Harvard Medical School, 77 Avenue Louis Pasteur, Boston, MA 02115, USA

Summary

Vibrio cholerae is the causative agent of the diarrheal disease cholera. Although many *V. cholerae* virulence factors have been studied, the role of interbacterial interactions within the host gut and their influence on colonization are poorly understood. Here, we utilized the conjugative properties of a *Vibrio*-specific plasmid to serve as a quantifiable genetic marker for direct contact among *V. cholerae* cells in the infant rabbit model for cholera. In conjunction, we also quantified contact-dependent type 6 secretion system (T6SS)-mediated killing of co-infecting *V. cholerae* strains. Tracking these interbacterial interactions revealed that most contact-dependent cell-cell interactions among *V. cholerae* occur in specific intestinal microenvironments, notably the distal small intestine and cecum, and that the T6SS confers a competitive advantage within the middle small intestine. These results support a model for *V. cholerae* gut colonization that includes microenvironments where critical microbial-host and bacterial-bacterial interactions occur to facilitate colonization by this pathogen.

eTOC blurb

To examine *V. cholerae* bacterial population structure within the host intestine, Fu et al. use DNA conjugation as a genetic reporter for bacterial cell-cell contacts along with measurements of antagonistic T6SS-mediated interactions. These observations reveal that contact-dependent cell-cell interactions and the T6SS play specific roles in distinct intestinal microenvironments.

*Correspondence: john_mekalanos@hms.harvard.edu.
[2]These authors contributed equally
[3]Lead Contact

Author Contributions

Conceptualization and Methodology, Y.F., B.T.H., and J.J.M; Investigation, Y.F. and B.T.H.; Writing – Original Draft, B.T.H.; Writing – Review & Editing, Y.F., B.T.H., and J.J.M; Funding Acquisition, J.J.M.

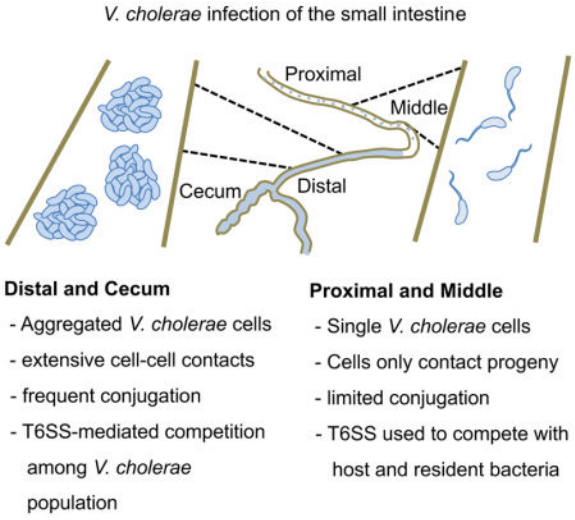

Introduction

The bacterium *V. cholerae* is the causative agent of cholera, a severe diarrheal disease that continues to be a significant cause of death in developing countries (Chin et al., 2011; Harris et al., 2012). Our current understanding of the *V. cholerae* infection process comes from studies of infection in neonatal rabbits (Ritchie et al., 2010) and mice (Gardel and Mekalanos, 1996) as well as human volunteers (Herrington et al., 1988; Lombardo et al., 2007). Transposon mutagenesis and deep sequencing analysis have identified genes for several colonization factors and their regulators (Fu et al., 2013; Kamp et al., 2013; Peterson and Mekalanos, 1988).

However, *V. cholerae* population dynamics within animal and human hosts has remained largely unexplored. Early work showed that the distribution of viable cells within the mouse intestine is variable and influenced by TCP and lipopolysaccharide O antigen (Angelichio et al., 1999). Attempts have also been made to visualize fluorescently-labeled bacteria during animal infections (Millet et al., 2014). However, these studies only provide a small snapshot of bacterial localization and are blind to changes in or movement of the bacterial population within the host over time.

Sequence Tag-based Analysis of Microbial Populations (STAMP) technology (Abel et al., 2015) opened the door to studying in vivo bacterial populations by allowing investigators to infer changes in population localization without direct visualization of the bacteria. However, STAMP cannot provide insights on bacterial cell-cell interactions taking place within the expanding infection, e.g. indirect interactions through host stimulation (Buffie and Pamer, 2013), cell-cell signaling through processes like quorum sensing (Papenfort and Bassler, 2016), or contact-dependent antagonism like the Type 6 Secretion System (T6SS) (Pukatzki et al., 2006).

T6SS is a dynamic nanomachine (Basler et al., 2012) that can suppress the growth or kill sensitive bacterial cells by contact dependent transfer of toxic effector proteins (MacIntyre et

al., 2010; Russell et al., 2011). While T6SS plays a role in disease by some non-O1/non-O139 *V. cholerae* strains (Ma et al., 2009), it appears to be dispensable for intestinal colonization by the 7th pandemic El Tor *V. cholerae* strain in the neonatal rabbit model of cholera (Fu et al., 2013). T6SS is nevertheless actively expressed and fully functional in the host intestine (Fu et al., 2013). Additionally, because T6SS is involved in antagonistic interactions with the intestinal microbiota of mice (Anderson et al., 2017; Sana et al., 2016), we wondered whether the T6SS might play a role in population dynamics by influencing the *V. cholerae* colonization process.

A complication of studying T6SS-mediated bacterial interactions is that they typically result in elimination of a subset of the population being investigated (Basler et al., 2013; Ho et al., 2013). Inherently lethal events can become challenging to address during infection because of confounding variables such as host-dependent killing through innate immune processes or in vivo growth rate variation.

To address these challenges, we developed a genetic assay to evaluate bacterial contact that takes advantage of the conjugative properties of a *Vibrio*-specific plasmid, P-factor (Datta et al., 1973), to serve as an indicator for *V. cholerae* populations that have come into direct contact with each other during the infection process. This analysis revealed that there are different microenvironments in the intestine where cell-cell bacterial interactions occur. The T6SS confers a competitive advantage for *V. cholerae* in some of these sites by either targeting the host or resident microbiota. We also we show that horizontal gene transfer (HGT) mediated by DNA conjugation is substantially more efficient in vivo than bacteria occupying an equivalent surface area in vitro, suggesting that the host environment may promote HGT among infectious *V. cholerae* populations.

Results

Temporal and anatomical stratification of T6SS-dependent colonization defects

The T6SS of *V. cholerae* C6706 is active in vivo in an 18–20 hour neonatal rabbit infection model (Fu et al., 2013). We previously reported a competitive advantage for *V. cholerae* carrying a fully functional T6SS over isogenic strains lacking immunity to *V. cholerae* T6SS effectors (Fu et al., 2013). To understand how the T6SS confers this competitive advantage, we investigated different anatomical locations within the small intestine at different stages of the infection. Consistent with previous studies (Abel et al., 2015), we observed that *V. cholerae* undergoes three basic stages of infection (Figure 1A). At the early stage (3 hr post-infection), *V. cholerae* was evenly distributed throughout the small intestine and cecum with approximately 10^6 CFU per cm of tissue. During the middle stage (6–12 hr post-infection), a 'bottlenecking' event occurred in the PSI and MSI as bacterial loads dropped to 10^5 CFU per cm of tissue. By the late stage (18 hr post-infection), the population in the PSI and MSI expanded to reach 10^9 CFU per cm of tissue throughout the small intestine.

We determined the competitive advantage for having a T6SS, focusing on the 3-, 6-, and 18-hr time points (Figure 1B). At 3 hr post-infection, we observed a 5-fold competitive advantage in the DSI for the T6SS$^+$ strain (C6706 *lacZ*) compared to an isogenic T6SS$^-$ mutant (C6706 *vipA tsiV3*). This competitive advantage increased to 100-fold by 18 hr post-

infection. In contrast, no competitive advantage was observed in the MSI at 3 hours and only 2-fold advantage emerged after 6 hours, followed by a 20-fold advantage at 18 hours. Together, these data suggest that at the early stage of infection, although bacteria are present throughout the intestine, T6SS-mediated interbacterial killing is limited to the DSI, implying that bacterial cells undergo direct contact with each other primarily in the DSI.

DNA conjugation as a measure of bacterial cell-to-cell contact during infection

It is difficult to infer from the above data whether the competitive advantage for T6SS$^+$ *V. cholerae* is due to inter-*Vibrio* T6SS killing or some secondary interaction with the host or other commensal bacteria. To distinguish between these possibilities, we needed to assay for bacterial contact without affecting the viability of the population being measured. Type 4 secretion system (T4SS)-mediated bacterial conjugation is another contact-dependent process that involves direct DNA transfer of genetic material between contacting bacterial cells (Christie and Cascales, 2005). As such, acquisition of a conjugative element by a recipient cell implies direct contact with a conjugative donor cell. We used J13, a variant of the *Vibrio*-specific conjugative plasmid P-factor carrying a Tn1 transposon insertion conferring resistance to carbenicillin, to measure the relative rates of cell-cell contact during *V. cholerae* infection. This plasmid is fully de-repressed for conjugation between *V. cholerae* cells (Johnson and Romig, 1979).

We used differentially marked (*lacZ*$^{+/-}$) but otherwise isogenic strains of *V. cholerae* C6706 and transferred J13 into the LacZ$^-$ strain. We then infected infant rabbits with a 1:1 mixture of these strains and recovered CFU from the rabbits after 3 to 18 hours, plating on separate differential media with streptomycin to select for *V. cholerae*, X-gal to differentiate between the LacZ$^+$ and LacZ$^-$ strains, and carbenicilin to select for transconjugates carrying J13 (Figure S1A). Conjugation efficiency was determined by dividing the CFU of recovered transconjugants (Figure S1B) by the total CFU of recipient cells. Carriage of J13 did not cause a significant colonization defect (Figure S1C). We confirmed that transconjugants were not the result of lysis and subsequent transformation events (Veening and Blokesch, 2017) by observing no transfer events when J13 was replaced with a high-copy number plasmid lacking conjugative properties (Figure S1D). Since overall levels of colonization were low at early times (Figure 1A), we also measured the minimal threshold of colonization at which conjugation could be detected. We determined that at least 10^5 CFU/cm of tissue needed to be isolated in the final population to consistently detect transconjugants in intestinal extracts (Figure S1E). Animals with fewer than 10^5 CFU/cm of tissue were considered to be not colonized and were excluded from evaluation.

We next sought to correlate bacterial conjugation with the cell-to-cell contacts required for T6SS killing by observing these events at the same time. We used a T6SS$^+$ strain (C6706 *lacZ*) as the conjugative donor and a strain that was sensitive to T6SS killing (C6706 *vipA tsiV3*) as the recipient. We then co-infected with these two strains and measured the final CFU of each, as well as the number of transconjugants in extracts derived from infected animals. When the recipient was sensitive to T6SS (Figure 2A), we almost never observed transconjugants in the animal extracts (Figure 2B). In each case we confirmed that there were at least 10^5 CFU/cm of tissue (Figure 2C), indicating that the lack of observed

conjugation was not due to insufficient bacterial load. These data suggest that recipient cells were killed either before they could acquire the conjugative plasmid or shortly after they acquired the plasmid. The timeframe analyzed is concordant with the amount of time required for a bacterium to be killed by T6SS which occurs within minutes of cell-cell contact (Basler et al., 2013).

We next determined the conjugation efficiency at the same time points and anatomical locations previously analyzed for T6SS-dependent killing (Figure 1B). We detected successful conjugation events in 5% of potential recipients in the DSI and cecum after just 3 hours post-challenge. This degree of conjugation was maintained through 12 hours but by 18 hours, the total conjugation efficiency increased to 10% (Figure 3A). No conjugation was detected in the MSI at 3 hours, consistent with the lack of an observed competitive advantage for T6SS$^+$ donors in the MSI at this time point. Colonization of the PSI at the early time points was too low to detect conjugation, but at 12 and 18 hours, the conjugation rate occurring in the PSI matched that observed in the MSI. Interestingly, in the PSI and MSI, only a small amount of conjugation was detected during the middle and late stages of infection (less than 1%). This result suggests that the bacteria initially colonizing these regions do not come into direct contact with each other, despite the fact that these anatomical sites are colonized with similar levels of bacteria as the DSI and cecum (Figure 1A).

It was previously reported that at late stages of infection (12–18 hr post challenge), the low population diversity in the PSI from the colonization bottleneck is replaced by a population of cells that reflects the high diversity present in the DSI, suggesting that *V. cholerae* initially colonizing the DSI travel retrograde through the intestine to eventually colonize the PSI (Abel et al., 2015). We observed that only ~1% or less of the potential recipient cells recovered from the PSI and MSI carry the J13 conjugative element whereas 5–10% of the bacteria present in the DSI acquired this element during the same timeframe (Figure 3A). If the population in the DSI ultimately colonizes the PSI at later time points, then at least 5% of the recipient cells derived from the PSI should carry the conjugative plasmid. Our data suggest a further stratification of the *V. cholerae* intestinal population such that the cells that are undergoing cell-to-cell contacts remain in the DSI, while cells not undergoing these contacts (e.g., luminal planktonic cells) are ultimately the ones responsible for the retrograde colonization of the PSI previously described (Abel et al., 2015).

V. cholerae T6SS plays a role in the colonization of the MSI

Our inability to detect direct cell-cell contact between *V. cholerae* cells in the MSI presents an apparent contradiction with our earlier observation that T6SS$^+$ strain (C6706 *lacZ*) had a competitive advantage over its T6SS-sensitive isogenic *tsiV3* mutant in this intestinal location (Figure 1B) as it is presumably impossible for T6SS-sensitive cells to be killed by a T6SS$^+$ strain if they do not come into direct contact. This discrepancy can be explained by considering the properties of the strains we used in these assays. Because the T6SS is known to be expressed and active in vivo (Fu et al., 2013; Mandlik et al.), we used a T6SS-sensitive strain (C6706 *vipA tsiV3*) that was also defective in its own T6SS apparatus. Using this strain avoided confounding self-killing effects but also eliminated potential interactions with

resident commensal organisms. In other words, the competitive advantage of having a functional T6SS might not be due to interactions among *Vibrio* cells but rather due to *Vibrio* cells interacting with the host or its resident microbiota through its T6SS. To test this hypothesis, we repeated the competition experiment using differentially marked T6SS$^+$ (C6706) and T6SS$^-$ (C6706 *vipA lacZ*) strains that retained full T6SS immunity to each other. We specifically measured the competitive index of these two strains at the late stage of infection to probe for any detectable selective advantage that the T6SS$^+$ strain had independent of its ability to kill sensitive sister cells (Figure 3B). We found that the T6SS$^+$ strain retained a 5-fold advantage for colonization of the MSI, but no advantage in the DSI or cecum.

We also addressed whether the primary anti-eukaryotic T6SS effector is the actin-crosslinking domain of VgrG-1, which is responsible for T6SS-dependent cytotoxicity toward macrophages (Ma et al., 2009; Pukatzki et al., 2007) was involved in the enhanced colonization of the T6SS$^+$ strain but found no evidence for this hypothesis (Figure S2). Thus, the colonization advantage displayed by T6SS$^+$ strains may be due to antibacterial activity toward yet-undefined members of the resident microbiota competing with *V. cholerae* for a specific intestinal location. A recent study suggests that commensal bacteria antagonistic to *V. cholerae* exist in humans (Hsiao et al., 2014), but it is not known whether these organisms are targets for T6SS activity in vivo.

V. cholerae cell-cell contact occurs within a restricted colonization area during infection

TCP is an important factor for *V. cholerae* aggregation and intestinal attachment in vivo (Krebs and Taylor, 2011; Taylor et al., 1987). However, despite being unable to stably colonize the rabbit intestine, TCP$^-$ mutants of *V. cholerae* still engaged in a significant degree of DNA conjugation in the DSI and cecum (Figure S3). As such, we wondered whether there might be some other factor responsible for bringing *V. cholerae* cells into close cell-to-cell contact. One possibility is that only limited locations on the mucosal surface are available for colonization and that this effectively brings cells together in close contact. To understand the effect of cell density on conjugation rates, we measured conjugation rates as a function of cell density.

Assuming the intestine is a perfect cylinder, which is an underestimate of the actual intestinal surface area because of mucosal invaginations, and a lumen diameter of 1 mm, we typically collected approximately 1.2×10^5 bacteria per cm^2 of intestinal surface (Figure 4A). We spotted incrementally increasing numbers of bacteria on an equivalent surface area of LB agar and calculated the rate of bacterial conjugation over 3 hours (Figure 4B). We observed that even when 100-fold higher concentrations of bacteria are spotted on an agar surface, the rate of conjugation is orders of magnitude lower than that observed during in vivo infection. We also wondered whether this property would also hold true for other conjugative elements. The SXT element (Waldor et al., 1996) is an epidemiologically relevant integrative conjugative element conferring resistance to trimethoprim-sulfamethoxazole and is present in the strain responsible for the recent cholera outbreak in Haiti, KW3 (Chin et al., 2011). We measured the conjugation rate of the SXT element using KW3 as the donor and C6706 as the recipient and observed an in vivo conjugation rate of ~1

per 10^5 recipients, which like J13, is orders of magnitude higher than equivalent measurements under in vitro conditions (Figure 4C). While it is possible that this elevated conjugation rate can be partially explained by up-regulation the conjugation machinery in vivo, that we can observe this behavior in two very different conjugative elements suggests that factors beyond derepression are also relevant. One possibility is that microenvironments in the host force close physical proximity of colonizing cells through, for example, adherence to epithelial cell receptors that are only displayed on cells in patches of high density. If true, we predicted that filling these microenvironments with one strain would prevent super-infection colonization by another. To test this hypothesis, we set up a sequential challenge model. We infected infant rabbits with a prototype live attenuated vaccine *V. cholerae* strain Peru-NT (Rui et al., 2010) lacking the genes required for toxin production, and followed it 6 hours later with super-infection with the wild type C6706 strain. The toxin-defective strain was used in the primary challenge to avoid potential complications arising from manifestation of disease symptoms. After 18 hours, we measured the total CFU of each strain at different anatomical locations (Figure 4D). As expected, we recovered 2-logs fewer CFU of the superinfecting C6706 strain. The lack of colonization by the superinfecting strain was observed consistently at all anatomical locations. We interpret these data to mean that once *V. cholerae* cells have colonized the small intestine, the "colonization vacancies" are occupied and become unavailable for additional new *V. cholerae* cells to occupy.

We next asked if we could detect cell-cell interactions between the superinfecting C6706 cells and initially colonizing Peru-NT cells. These cell-cell contacts would be necessary for other contact-dependent interactions, like T6SS-mediated killing, to occur. We measured the rate of conjugation between these two bacterial populations using the initial colonizer as the donor. In the MSI there was little detectable conjugation, suggesting that bacteria entering the MSI almost completely bypass the colonizing bacteria from the primary infection, while in the DSI and cecum about 0.1% of recipients received the plasmid, compared to the 8% observed during co-infection (Figure 4E). Although conjugation is detected, the per-recipient rate is nearly 100-fold lower than if the bacteria were introduced to the animal at the same time. These data are consistent with the hypothesis that the primary sites of intestinal colonization at 6 hours are occupied and become largely inaccessible to the superinfecting strain. A similar conclusion was recently reached independently using a different live attenuated vaccine prototype (Hubbard, Billings, Dorr, Sit, Warr, Kuehl, Kim, Delgado, Mekalanos, Lewnard, and Waldor, submitted for publication).

Discussion

In this work, we dissected the temporal and spatial population dynamics of *V. cholerae* during infection in the neonatal rabbit model while specifically addressing the difficult challenge of understanding the role of bacterial cell-cell interactions that occur in vivo. By using T6SS-dependent killing and plasmid conjugations, we were able to gain insight into when and where homologous interbacterial interactions occur in the intestine. From these observations, we propose a detailed model for the intestinal colonization process and a potential role of the T6SS in that process as a virulence factor of *V. cholerae*.

After passing through the stomach, *V. cholerae* cells enter the intestinal tract and distribute themselves evenly throughout the small intestine (Figure S4A). Most cells appear to be planktonic at this early phase, as they do not show signs of cell-cell contact. However, specifically in the DSI and cecum, a subset of the population engages in direct cell-to-cell interactions. These interactions occur in the absence of TCP, a factor required for in vivo aggregation and attachment. By the middle stage of infection, population restriction occurs in the PSI and MSI (Figure S4B). This restriction could be the result of host responses that actively eliminate bacteria, competition with established commensal microbiota, or simply niche selection where, for example, non-adherent bacteria pass through into the DSI and cecum. Our data show that having a functional T6SS helps *V. cholerae* colonize the MSI and PSI. We imagine that single cells that pass the restrictions of the PSI and MSI are able to grow into collections of isogenic daughter cells that do not interact with other *V. cholerae* cells (Figure S4C). After the population restriction in the PSI, bacteria travel retrograde from more distal intestinal locations to repopulate the PSI (Abel et al., 2015). These relocating bacteria come from a planktonic sub-population that did not engage in contacts with other *V. cholerae* cells.

Quantifying in vivo conjugation events represents a new tool to track individual members of a pathogenic species in a complex bacterial community. While conjugation has been used to tag genetically interacting members of complex microbial communities (Stecher et al., 2012), conjugation was not used to understand the dynamics of a single pathogenic bacterial species in vivo. Our methodology may be applicable to understanding other systems where cell-cell contact may be critical but would be less useful for studying cell-cell interactions involving diffusable molecules (Papenfort and Bassler, 2016).

It is notable that phage transduction by the CTX phage is greatly enhanced under in vivo conditions (i.e., during infant mice infection) (Waldor and Mekalanos, 1996). Although the receptor for CTX phage is TCP and the genes for this colonization factor are known to be highly expressed in vivo (Angelichio et al., 1999; Lee et al., 1999; Mandlik et al., 2011), our data suggest that the enhanced in vivo transfer of accessory genetic elements such as CTX phage in vivo may have another explanation. Thus, close proximity of cells caused by undefined host factors may enable HGT generally to occur more efficiently in vivo than in the aquatic environment. Inflammation can bloom enteric bacteria that can use alternative electron acceptors (Winter et al., 2010), which produce measurable changes in HGT in vivo (Stecher et al., 2012). Thus, the host milieu during infection may provide physical, chemical, regulatory and nutrition factors that influence cell-cell interactions and HGT, which has potential epidemiological implications for the spread of antibiotic resistance and virulence factors.

We observed that the T6SS confers a competitive advantage for colonization specifically in the PSI and MSI. This advantage does not depend on the anti-eukaryotic effector VgrG1, suggesting that T6SS may be acting on resident commensal bacterial species. Recent work in our laboratory has confirmed that T6SS is indeed capable of killing commensal organisms in the infant mouse model for cholera and that this antibacterial activity stimulates *V. cholerae* colonization (Zhao, Caro, Robins, and Mekalanos, submitted for publication). Furthermore, a human commensal species has been found to antagonize *V. cholerae*

colonization in previously gnotobiotic mice (Hsiao et al., 2014), suggesting that T6SS may be important depending on the commensal species present in any given animal species. Our finding that T6SS is a colonization factor in the neonatal rabbit is a novel observation that was likely missed in earlier studies (Fu et al., 2013) because these did not address the spatial and temporal aspects of the colonization process in relation to virulence factor requirements.

Bacteria in different parts of the small intestine experience likely encounter distinct challenges. Our work suggests that *V. cholerae* may have evolved its colonization strategy to optimize its survival in different locations. For example, we showed that *V. cholerae* initially colonizes the PSI and MSI as single cells, which may be reflective of the need for chemotaxis or motility to pass though the mucosal layer and/or to access anatomical sites that are mechanically difficult to reach (e.g., the brush border epithelium that is protected by glycocalyx or the deep crevices of the intestinal crypts). As single cells, it is "every man for himself," and as a result, having a functional T6SS to eliminate resident commensal bacteria may be helpful. On the other hand, cells colonizing the DSI and cecum form groups with bacteria present in the initial inoculum. As a result, in the DSI and cecum, bacteria with functional T6SSs might be trans-complementing the T6SS mutants, effectively masking their colonization defect.

In this work, we found that localized spatial restrictions on *V. cholerae* colonization not only serve to promote inter-cellular interactions but also impact *V. cholerae* colonization dynamics. Thus, a superinfecting strain does not contact a strain that was initially given the chance to colonize. In this regard, it is exciting to note that a newly developed, live attenuated *V. cholerae* vaccine is capable of protecting against disease within hours of its initial administration (Hubbard, Billings, Dorr, Sit, Warr, Kuehl, Kim, Delgado, Mekalanos, Lewnard, and Waldor, submitted for publication). Thus, understanding how to block the earliest steps in *V. cholerae* colonization may have potential applications in the development of effective cholera vaccines and probiotics.

Star Methods

CONTACT FOR REAGENT AND RESOURCE SHARING

Further information and requests for resources and reagents should be directed to and will be fulfilled by the Lead Contact, John Mekalanos (john_mekalanos@hms.harvard.edu).

EXPERIMENTAL MODEL AND SUBJECT DETAILS

Ethics statement—All infant rabbit experiments in this project were performed with the protocol approved by the Harvard Medical School Office for Research Protection Standing Committee on Animals in accordance to NIH guidelines. Harvard Medical School animal management program is accredited by the Association for the Assessment and Accreditation of Laboratory Animal Care International (AAALAC International). The institution also accepts as mandatory of the PHS Policy on Humane Care and Use of Laboratory Animals by Awardee Institutions and NIH Principles for the Utilization and Care of Vertebrate Animals Used in Testing, Research, and Training. The office of Laboratory Animal Welfare (OLAW) has the approved Assurance of Compliance (A3431-01) on file.

Vertebrate animals—The “infant” (neonatal) rabbit model assays used in this study were adapted from those previously described (Ritchie et al., 2010; Shin et al., 2011). Litters of 2-day-old New Zealand White infant rabbits were obtained from commercial breeders (Pine Acre Rabbitry, Norton, MA; Charles River Laboratories, Cambridge, MA) and housed together with the adult female for the duration of each experiment in a BL2 animal facility room. Following oral gavage, infected infant rabbits were monitored every 5 hours for signs of dehydration and loss of body weight. Animals exhibiting severe disease were immediately euthanized.

Bacterial Strains—The *V. cholerae* strains used in this study were C6706, a 1991 Peruvian isolate, KW3, a 2010 Haitian El Tor O1 clinical isolate (Chin et al., 2011), and Peru-NT live attenuated vaccine strain (Rui et al., 2010). Bacteria were cultured in Luria Broth (LB) for liquid and on LB agar at 37 C. Plasmid J13 (Johnson and Romig, 1979) was conjugated from a *V. cholerae* MAK757 strain found in our laboratory collection into C6706 and Peru-NT for use in this study.

METHOD DETAILS

Bacterial Strains and Growth Conditions—Strains used in this study are listed in the key resources table. C6706, a 1991 Peruvian isolate, and KW3, a 2010 Haitian El Tor O1 clinical isolate (Chin et al., 2011), were the *V. cholerae* strains used in this study for T6SS killing and conjugation assays. For superinfection experiments, the initial strain was the Peru-NT live attenuated vaccine strain (Rui et al., 2010). Bacteria were cultured in Luria Broth (LB) for liquid and on LB agar at 37 C. Antibiotics were used at the following concentrations where necessary: streptomycin (Sm: 100 μg/ml), kanamycin (Kan: 50 μg/ml), carbenicillin (Carb: 75 μg/ml) and trimethoprim (Trim: 30 μg/ml). X-gal (40 μg/ml) was used for LacZ Blue/White screening. Plasmid J13 (Johnson and Romig, 1979) was conjugated from a *V. cholerae* MAK757 strain found in our laboratory collection into C6706 and Peru-NT for use in this study. The DNA of the J13 plasmid was sequenced to confirm a Tn1 insertion conferring Carb resistance.

Bacterial Mutant Construction—*V. cholerae* mutants used in this study were constructed as previously described (Metcalf et al., 1996; Miller and Mekalanos, 1988). Briefly, genomic DNA surrounding the target genes was amplified by PCR and cloned into suicide vectors pWM91 or pDS132, then transformed into SM10 λpir, then mated with *V. cholerae* C6706 or C6706 *lacZ*. Double crossovers successfully deleting target genes were then confirmed by PCR and sequencing.

Neonatal rabbit model—*V. cholerae* strains were initially grown overnight on LB-agar plates at 37 C. A fresh colony of each strain was inoculated in LB and incubated at 300 rpm at 37 C for 3 hours. Cultures were adjusted to OD_{600} = 1.0, pelleted at 8000 rcf for 5 minutes, re-suspended in 2.5% Sodium Bicarbonate Buffer to a final concentration of 2×10^8 CFU/ml. For each experimental group, 2-day-old neonatal rabbits (no specific sex requirement) were given antacid treatment with Zantac (2 μg/g of body weight) by intraperitoneally injection 3 hours prior to orogastric inoculation of *V. cholerae* strains. At the experimental endpoint (3, 6, 12 or 18 hours post infection), animals were sacrificed after

anesthetized by inhalation of isofluorane by heart injection of 2.5 mL KCl solution. 1 cm of tissue from different intestinal sections (Upper Small Intestine; Middle Small Intestine; Distal Small Intestine; Cecum) were collected from each animal and homogenized in 1 mL of sterile PBS using a beat-beater (BioSpec Products, Inc.) for bacterial recovery and CFU colony counting. For superinfection experiments, animals were infected as described above. After 3 hours, a second dose of Zantac was administered, followed by secondary infection 6 hours after the first infection.

In vivo competition assays and conjugation assays—Inoculum strains for the experimental infant rabbits were prepared as described above. Predator and prey strains (for competition assays), or donor and recipient strains (for conjugation assays) were 1:1 mixed together in 2.5% sodium bicarbonate buffer and inoculated into a 2-day-old New Zealand white rabbit kits. Kits were sacrificed, dissected, and a 1cm of each intestinal section sample was removed and homogenized in 1 ml of 1xPBS. Serial dilutions were plated on LB agar with Sm and X-gal to enumerate the output ratio of the wild type and mutant strain. The C.I. for each mutant is defined as the input ratio of mutant/WT strain divided by the output ratio of mutant/WT strain. For in vivo conjugation assays, successful conjugants (blue colonies) were selected by LB agar contained Sm, Carb and X-gal. Estimated recipients were counted by donors (white colonies) multiplied by the input ratio of recipient/donor. Conjugation efficiency is defined as the number of transconjugants divided by total estimated recipients. A minimum of six rabbits were assayed for each group.

QUANTIFICATION AND STATISTICAL ANALYSIS

Statistical Methods—Statistical significance was determined by student's *t* test between indicated groups using GraphPad Prism. Data presented represent the mean with error bars signifying the standard error of the mean. For infection experiments, animals where less than 10^5 CFU/cm tissue were collected, the animals were deemed to have failed to be colonized and the entire animal was excluded from all analysis. For all data sets, except where otherwise specified, an *n* of at least 5 animals with sufficient colonization were used.

Supplementary Material

Refer to Web version on PubMed Central for supplementary material.

Acknowledgments

We thank the members of the Mekalanos and Waldor labs for helpful discussions regarding this project. This work was supported by National Institute of Allergy and Infectious Diseases Grant AI-01845 (to J.J.M.).

References

Abel S, Abel zur Wiesch P, Chang HH, Davis BM, Lipsitch M, Waldor MK. Sequence tag-based analysis of microbial population dynamics. Nature methods. 2015; 12:223–226. 223 p following 226. [PubMed: 25599549]

Anderson MC, Vonaesch P, Saffarian A, Marteyn BS, Sansonetti PJ. Shigella sonnei Encodes a Functional T6SS Used for Interbacterial Competition and Niche Occupancy. Cell host & microbe. 2017; 21:769–776. e763. [PubMed: 28618272]

Angelichio MJ, Spector J, Waldor MK, Camilli A. Vibrio cholerae intestinal population dynamics in the suckling mouse model of infection. Infection and immunity. 1999; 67:3733–3739. [PubMed: 10417131]

Basler M, Ho BT, Mekalanos JJ. Tit-for-tat: type VI secretion system counterattack during bacterial cell-cell interactions. Cell. 2013; 152:884–894. [PubMed: 23415234]

Basler M, Pilhofer M, Henderson GP, Jensen GJ, Mekalanos JJ. Type VI secretion requires a dynamic contractile phage tail-like structure. Nature. 2012; 483:182–186. [PubMed: 22367545]

Buffie CG, Pamer EG. Microbiota-mediated colonization resistance against intestinal pathogens. Nat Rev Immunol. 2013; 13:790–801. [PubMed: 24096337]

Cameron DE, Urbach JM, Mekalanos JJ. A defined transposon mutant library and its use in identifying motility genes in Vibrio cholerae. Proceedings of the National Academy of Sciences of the United States of America. 2008; 105:8736–8741. [PubMed: 18574146]

Chin CS, Sorenson J, Harris JB, Robins WP, Charles RC, Jean-Charles RR, Bullard J, Webster DR, Kasarskis A, Peluso P, et al. The origin of the Haitian cholera outbreak strain. The New England journal of medicine. 2011; 364:33–42. [PubMed: 21142692]

Christie PJ, Cascales E. Structural and dynamic properties of bacterial type IV secretion systems (review). Mol Membr Biol. 2005; 22:51–61. [PubMed: 16092524]

Datta A, Parker CD, Wohlhieter JA, Baron LS. Isolation and characterization of the fertility factor P of Vibrio cholerae. Journal of bacteriology. 1973; 113:763–771. [PubMed: 4690964]

Fu Y, Waldor MK, Mekalanos JJ. Tn-Seq Analysis of Vibrio cholerae Intestinal Colonization Reveals a Role for T6SS-Mediated Antibacterial Activity in the Host. Cell host & microbe. 2013; 14:652–663. [PubMed: 24331463]

Gardel CL, Mekalanos JJ. Alterations in Vibrio cholerae motility phenotypes correlate with changes in virulence factor expression. Infection and immunity. 1996; 64:2246–2255. [PubMed: 8675334]

Harris JB, LaRocque RC, Qadri F, Ryan ET, Calderwood SB. Cholera. Lancet. 2012; 379:2466–2476. [PubMed: 22748592]

Herrington DA, Hall RH, Losonsky G, Mekalanos JJ, Taylor RK, Levine MM. Toxin, toxin-coregulated pili, and the toxR regulon are essential for Vibrio cholerae pathogenesis in humans. J Exp Med. 1988; 168:1487–1492. [PubMed: 2902187]

Ho BT, Basler M, Mekalanos JJ. Type 6 secretion system-mediated immunity to type 4 secretion system-mediated gene transfer. Science. 2013; 342:250–253. [PubMed: 24115441]

Hsiao A, Ahmed AM, Subramanian S, Griffin NW, Drewry LL, Petri WA Jr, Haque R, Ahmed T, Gordon JI. Members of the human gut microbiota involved in recovery from Vibrio cholerae infection. Nature. 2014; 515:423–426. [PubMed: 25231861]

Johnson SR, Romig WR. Vibrio cholerae hybrid sex factor that contains ampicillin transposon Tn1. J Bacteriol. 1979; 137:531–536. [PubMed: 253004]

Kamp HD, Patimalla-Dipali B, Lazinski DW, Wallace-Gadsden F, Camilli A. Gene fitness landscapes of Vibrio cholerae at important stages of its life cycle. PLoS pathogens. 2013; 9:e1003800. [PubMed: 24385900]

Krebs SJ, Taylor RK. Protection and attachment of Vibrio cholerae mediated by the toxin-coregulated pilus in the infant mouse model. Journal of bacteriology. 2011; 193:5260–5270. [PubMed: 21804008]

Lee SH, Hava DL, Waldor MK, Camilli A. Regulation and temporal expression patterns of Vibrio cholerae virulence genes during infection. Cell. 1999; 99:625–634. [PubMed: 10612398]

Lombardo MJ, Michalski J, Martinez-Wilson H, Morin C, Hilton T, Osorio CG, Nataro JP, Tacket CO, Camilli A, Kaper JB. An in vivo expression technology screen for Vibrio cholerae genes expressed in human volunteers. Proceedings of the National Academy of Sciences of the United States of America. 2007; 104:18229–18234. [PubMed: 17986616]

Ma AT, McAuley S, Pukatzki S, Mekalanos JJ. Translocation of a Vibrio cholerae type VI secretion effector requires bacterial endocytosis by host cells. Cell host & microbe. 2009; 5:234–243. [PubMed: 19286133]

MacIntyre DL, Miyata ST, Kitaoka M, Pukatzki S. The Vibrio cholerae type VI secretion system displays antimicrobial properties. Proceedings of the National Academy of Sciences of the United States of America. 2010; 107:19520–19524. [PubMed: 20974937]

Mandlik A, Livny J, Robins WP, Ritchie JM, Mekalanos JJ, Waldor MK. RNA-Seq-based monitoring of infection-linked changes in Vibrio cholerae gene expression. Cell host & microbe. 2011; 10:165–174. [PubMed: 21843873]

Metcalf WW, Jiang W, Daniels LL, Kim SK, Haldimann A, Wanner BL. Conditionally replicative and conjugative plasmids carrying lacZ alpha for cloning, mutagenesis, and allele replacement in bacteria. Plasmid. 1996; 35:1–13. [PubMed: 8693022]

Miller VL, Mekalanos JJ. A novel suicide vector and its use in construction of insertion mutations: osmoregulation of outer membrane proteins and virulence determinants in Vibrio cholerae requires toxR. Journal of bacteriology. 1988; 170:2575–2583. [PubMed: 2836362]

Millet YA, Alvarez D, Ringgaard S, von Andrian UH, Davis BM, Waldor MK. Insights into Vibrio cholerae intestinal colonization from monitoring fluorescently labeled bacteria. PLoS pathogens. 2014; 10:e1004405. [PubMed: 25275396]

Papenfort K, Bassler BL. Quorum sensing signal-response systems in Gram-negative bacteria. Nature reviews Microbiology. 2016; 14:576–588. [PubMed: 27510864]

Peterson KM, Mekalanos JJ. Characterization of the Vibrio cholerae ToxR regulon: identification of novel genes involved in intestinal colonization. Infection and immunity. 1988; 56:2822–2829. [PubMed: 2902009]

Pukatzki S, Ma AT, Revel AT, Sturtevant D, Mekalanos JJ. Type VI secretion system translocates a phage tail spike-like protein into target cells where it cross-links actin. Proceedings of the National Academy of Sciences of the United States of America. 2007; 104:15508–15513. [PubMed: 17873062]

Pukatzki S, Ma AT, Sturtevant D, Krastins B, Sarracino D, Nelson WC, Heidelberg JF, Mekalanos JJ. Identification of a conserved bacterial protein secretion system in Vibrio cholerae using the Dictyostelium host model system. Proceedings of the National Academy of Sciences of the United States of America. 2006; 103:1528–1533. [PubMed: 16432199]

Ritchie JM, Rui H, Bronson RT, Waldor MK. Back to the future: studying cholera pathogenesis using infant rabbits. mBio. 2010:1.

Rui H, Ritchie JM, Bronson RT, Mekalanos JJ, Zhang Y, Waldor MK. Reactogenicity of live-attenuated Vibrio cholerae vaccines is dependent on flagellins. Proceedings of the National Academy of Sciences of the United States of America. 2010; 107:4359–4364. [PubMed: 20160087]

Russell AB, Hood RD, Bui NK, LeRoux M, Vollmer W, Mougous JD. Type VI secretion delivers bacteriolytic effectors to target cells. Nature. 2011; 475:343–347. [PubMed: 21776080]

Sana TG, Flaugnatti N, Lugo KA, Lam LH, Jacobson A, Baylot V, Durand E, Journet L, Cascales E, Monack DM. Salmonella Typhimurium utilizes a T6SS-mediated antibacterial weapon to establish in the host gut. Proc Natl Acad Sci U S A. 2016; 113:E5044–5051. [PubMed: 27503894]

Shin OS, Tam VC, Suzuki M, Ritchie JM, Bronson RT, Waldor MK, Mekalanos JJ. Type III secretion is essential for the rapidly fatal diarrheal disease caused by non-O1, non-O139 Vibrio cholerae. mBio. 2011; 2:e00106–00111. [PubMed: 21673189]

Stecher B, Denzler R, Maier L, Bernet F, Sanders MJ, Pickard DJ, Barthel M, Westendorf AM, Krogfelt KA, Walker AW, et al. Gut inflammation can boost horizontal gene transfer between pathogenic and commensal Enterobacteriaceae. Proceedings of the National Academy of Sciences of the United States of America. 2012; 109:1269–1274. [PubMed: 22232693]

Taylor RK, Miller VL, Furlong DB, Mekalanos JJ. Use of phoA gene fusions to identify a pilus colonization factor coordinately regulated with cholera toxin. Proceedings of the National Academy of Sciences of the United States of America. 1987; 84:2833–2837. [PubMed: 2883655]

Veening JW, Blokesch M. Interbacterial predation as a strategy for DNA acquisition in naturally competent bacteria. Nature reviews Microbiology. 2017

Waldor MK, Mekalanos JJ. Lysogenic conversion by a filamentous phage encoding cholera toxin. Science. 1996; 272:1910–1914. [PubMed: 8658163]

Waldor MK, Tschape H, Mekalanos JJ. A new type of conjugative transposon encodes resistance to sulfamethoxazole, trimethoprim, and streptomycin in Vibrio cholerae O139. Journal of bacteriology. 1996; 178:4157–4165. [PubMed: 8763944]

Winter SE, Thiennimitr P, Winter MG, Butler BP, Huseby DL, Crawford RW, Russell JM, Bevins CL, Adams LG, Tsolis RM, et al. Gut inflammation provides a respiratory electron acceptor for Salmonella. Nature. 2010; 467:426–429. [PubMed: 20864996]

Zheng J, Ho B, Mekalanos JJ. Genetic analysis of anti-amoebae and antibacterial activities of the type VI secretion system in Vibrio cholerae. PLoS One. 2011; 6:e23876. [PubMed: 21909372]

Highlights

- DNA conjugation can be used to track bacterial cell-cell contacts during infection.
- Sites of in vivo cell-cell contact correspond to sites of T6SS-mediated killing.
- *V. cholerae* T6SS contributes to colonization of the middle small intestine.
- DNA conjugation among *V. cholerae* occurs more efficiently in vivo than in vitro.

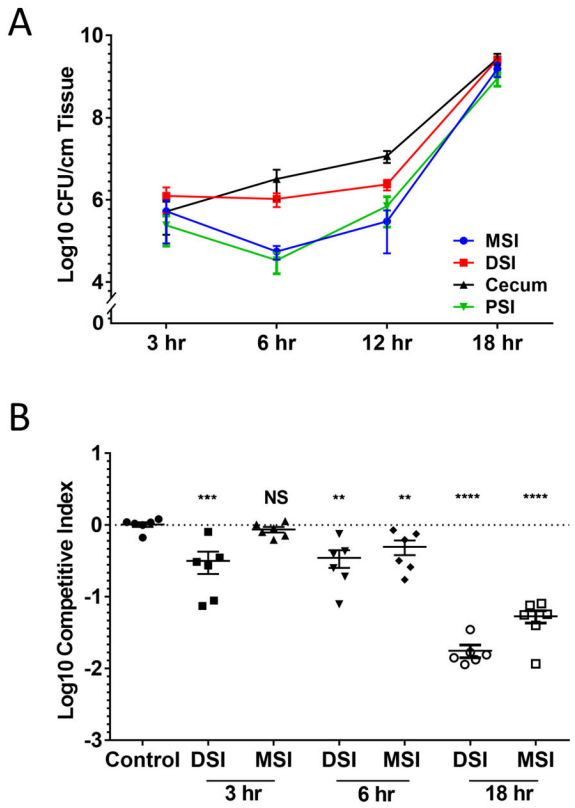

Figure 1. Spatial and temporal analysis of *V. cholerae* colonization

(A) *V. cholerae* population size was determined by counting colony forming units (CFU) present per cm of tissue in the proximal (PSI, Green), middle (MSI, Blue), distal (DSI, Red) small intestine, and cecum (Black) at 3, 6, 12, or 18 hr post infection. (B) In vivo competition experiments were performed between strains C6706 *tsiV3 vipA* (T6SS^{-} and T6SS-sensitive) and parental strain C6706 *lacZ* (T6SS^{+}). Bacteria were recovered from the MSI or DSI after 3, 6, and 18 hr. Control was a competition between wild type C6706 and C6706 *lacZ* in DSI after 18 hr. Each data point indicates the competitive index (C.I.) relative to wild type between the two strains for each experimental animal. Bars indicate mean and standard error. Significance was determined relative to the C.I. of the control group (NS - not significant, ** - $p < 10^{-2}$, *** - $p < 10^{-3}$, **** - $p < 10^{-4}$).

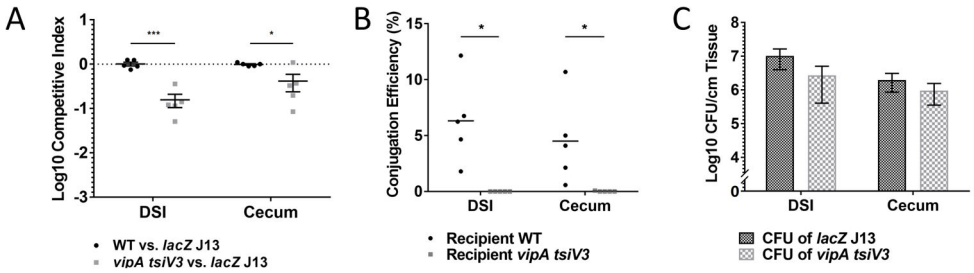

Figure 2. DNA conjugation correlates with T6SS killing in vivo

Competition assay was performed between donor C6706 *lacZ* J13 and recipient wild type C6706 or C6706 *vipA tsiV3* (T6SS^{-} and T6SS-sensitive). (A) Cells were recovered from the distal small intestine (DSI) and cecum at 3 hr post infection. Each data point indicates the C.I. relative to C6706 *lacZ* J13 for each experimental animal (B) Conjugation efficiency was determined for each group. (C) Donor and recipient bacterial population were above the 10^5 CFU/cm tissue minimum cell density thresholds. Bars indicate mean and standard error. Significance was determined by *t* test. * - $p < 5 \times 10^{-2}$, *** - $p < 10^{-3}$.

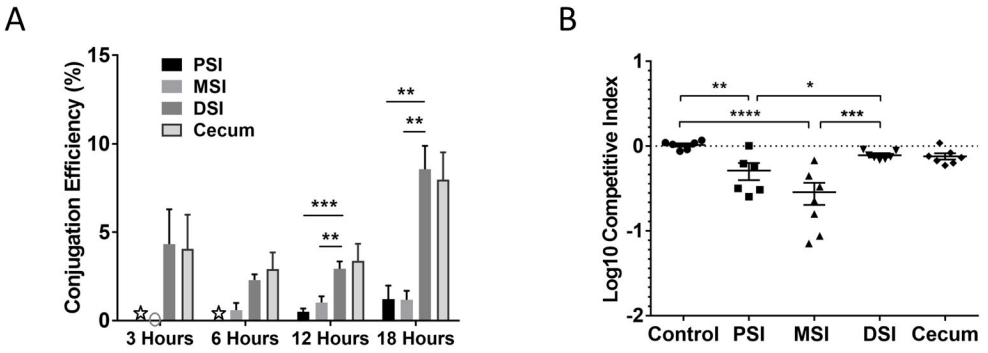

Figure 3. Analysis of conjugation efficiency at different anatomical locations reveals a role for T6SS in colonization

(A) Conjugation efficiency was determined for each tissue section (PSI, MSI, DSI, Cecum) at 3, 6, 12 and 18 hr post infection. Each column is the mean of at least 5 animals with bars indicating standard error. Gray circle indicates that no conjugants were detected, white stars indicate that the CFU in the PSI did not reach the 10^5 threshold to detect conjugation events. (B) Competition assays were performed comparing wild type C6706 (T6SS$^+$) to C6706 *vipA lacZ* (T6SS$^-$, T6SS-immune). Cells were recovered from the PSI, MSI, DSI or cecum of each experimental animal 18 hr post infection to determine the C.I. relative to the wild type. The control group is the C.I of C6706 and C6706 *lacZ* in the DSI 18 hr post infection. Bars indicate mean and standard error. Significance was determined by *t* test. * - $p < 5 \times 10^{-2}$, ** - $p < 10^{-2}$; *** - $p < 10^{-3}$, **** - $p < 10^{-4}$.

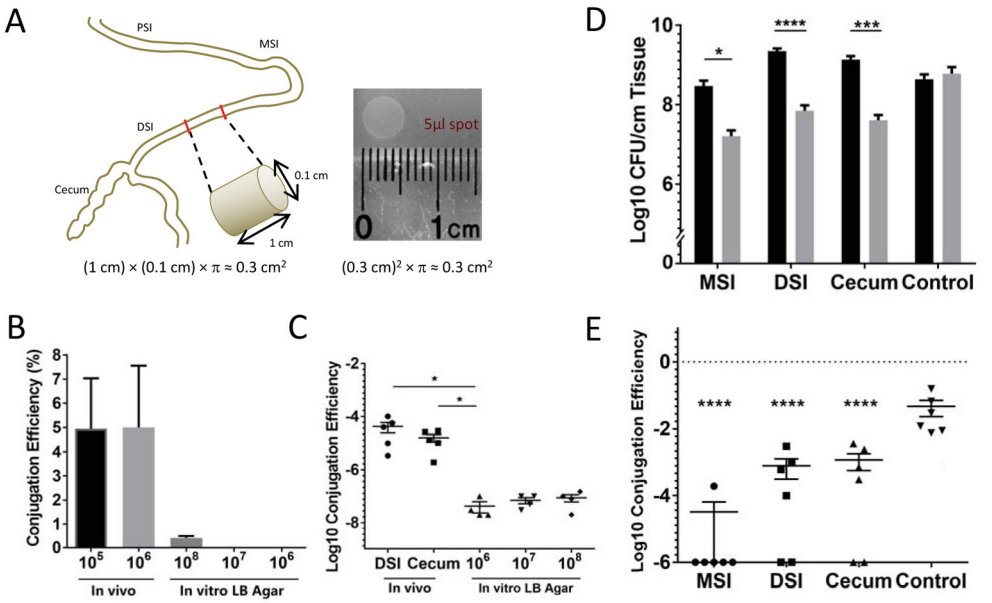

Figure 4. Colonizing *V. cholerae* bacteria fill specific colonization vacancies

(A) Schematic of a size estimation of the luminal surface area compared to an agar surface. (B) Mean conjugation efficiency of J13 between C6706 strains was determined for different bacterial densities at the time of recovery from either the DSI (in vivo) at 3 hr post infection or in vitro (LB Agar) 3 hr after being spotted onto a surface area equivalent to 1 cm intestine. Each column is the mean of 4 to 5 biological replicates. (C) Conjugation efficiency of the SXT element from donor strain KW3 to recipient C6706 *lacZ*::Tn after 18 hr was determined for the DSI, cecum and in vitro. Initial in vivo inoculum was 10^8 CFU with an equal number of donors and recipients. For in vitro conjugation, the indicated CFU were spotted on the agar surface. Significance was determined by *t* test. Bars represent the mean and standard error. (D and E) 6 rabbits were infected with Peru-NT J13. After 6 hours, wild type C6706 was used to superinfect the same animals. CFU counts and conjugation efficiency was determined from bacteria recovered from MSI, DSI, and cecum 24 hours after the initial inoculation. In the control group, no bacteria were present in the initial inoculation. Peru-NT J13 and C6706 were then inoculated together at the 6 hr time point. (D) Each column is the mean CFU/cm tissue recovered for Peru-NT J13 (Black) and C6706 (Gray) with error bars indicating standard error. Significance with determined by *t* test with * - $p < 0.05$, *** - $p < 10^{-3}$, **** - $p < 10^{-4}$. (E) Data points represent the conjugation efficiency of bacteria in each experimental animal with bars indicating mean and standard error. Significance with respect to the control group was determined by *t* test **** - $p < 10^{-4}$.

KEY RESOURCES TABLE

REAGENT or RESOURCE	SOURCE	IDENTIFIER
Bacterial Strains		
E. coli		
SM10 λpir	(Miller and Mekalanos, 1988)	*thi thr leu tonA lacY supE recA*::RP4-2-Tc::Mu *pirR6K*
V. cholerae		
C6706	Lab collection	*V. cholerae* El Tor biotype, Sm^R
C6706 *lacZ*	(Cameron et al., 2008)	*V. cholerae* El Tor biotype, Sm^R, *lacZ*
C6706 *lacZ*::Tn	(Cameron et al., 2008)	*V. cholerae* El Tor biotype, Sm^R, *lacZ*::TnFGL3 (Transposon insertion of the Kan^R and LacZ into the native LacZ gene)
YFJM2	(Fu et al., 2013)	C6706 *lacZ vipA*
YFJM4	(Fu et al., 2013)	C6706 *tsiV3 vipA*
YFJM6	This study	C6706 *lacZ vgrG1*
YFJM7	This study	C6706 *lacZ tcpA*
YFJM8	This study	C6706 *lacZ* J13
EC15669	(Cameron et al., 2008)	C6706 *tcpC*::TnFGL3
KW3	(Chin et al., 2011)	*V. cholerae* El Tor biotype, Sm^R, $Trim^R$
Peru NT	(Rui et al., 2010)	C6706 *lacZ ctxAB flgABCDE*
Peru NT / J13	This study	C6706 *lacZ ctxAB flgABCDE* pJ13 $Carb^R$
Plasmids		
pJ13	(Johnson and Romig, 1979)	P::Tn*1*
pdvgrG1	(Pukatzki et al., 2007)	Suicide vector for deletion of VgrG1
pdvipA	(Zheng et al., 2011)	Suicide vector for deletion of vipA
pdtcpA	This study	Suicide vector for deletion of tcpA
Experimental Models: Organisms/Strains		
2-5 day old	PineAcres Rabbitry; Charles	New Zealand White – Strain Code 052
infant rabbits	River Laboratories	
Chemicals, Peptides, and Recombinant Proteins		
Zantac	Covis	NDC: 24987-364-01
Software and Algorithms		
Prism 7	GraphPad	Statistical analysis software